electronics

MDPI

Article

Study of the Contributions of Donor and Acceptor Photoexcitations to Open Circuit Voltage in Bulk Heterojunction Organic Solar Cells

Douglas Yeboah and Jai Singh *

School of Engineering and Information Technology, Charles Darwin University, Darwin, NT 0909, Australia; douglas.yeboah@cdu.edu.au

* Correspondence: jai.singh@cdu.edu.au; Tel.: +61-8-8946-6811

Received: 1 September 2017; Accepted: 28 September 2017; Published: 3 October 2017

Abstract: One of the key parameters in determining the power conversion efficiency (PCE) of bulk heterojunction (BHJ) organic solar cells (OSCs) is the open circuit voltage (V_{OC}). The processes of exciting the donor and acceptor materials individually in a BHJ OSC are investigated and are found to produce two different expressions for V_{OC}s. Using the contributions of electron and hole quasi-Fermi levels and charge carrier concentrations, the two different V_{OC} expressions are derived as functions of the energetics of the donor and acceptor materials and the photo-generated charge carrier concentrations, and calculated for a set of donor-acceptor blends. The simultaneous excitation of both the donor and acceptor materials is also considered and the corresponding V_{OC}, which is different from the above two, is derived. The V_{OC} calculated from the photoexcitation of the donor is found to be somewhat comparable with that obtained from the photoexcitation of the acceptor in most combinations of the donor and acceptor materials considered here. It is also found that the V_{OC} calculated from the simultaneous excitations of donor and acceptor in BHJ OSCs is also comparable with the other two V_{OC}s. All three V_{OC}s thus derived produce similar results and agree reasonably well with the measured values. All three V_{OC}s depend linearly on the concentration of the photoexcited charge carriers and hence incident light intensity, which agrees with experimental results. The outcomes of this study are expected to help in finding materials that may produce higher V_{OC} and hence enhanced PCE in BHJ OSCs.

Keywords: open circuit voltage; power conversion efficiency; photoexcitation; donor material; acceptor material; bulk heterojunction organic solar cells

1. Introduction

Organic solar cells (OSCs) based on bulk heterojunction (BHJ) structure are promising candidates for the generation of clean, affordable electricity owing to their low fabrication cost compared to inorganic solar cells [1,2]. Recent research efforts into the development of new donor-acceptor blends have led to a significant improvement in the power conversion efficiency (PCE) of OSCs, above 11% [3–6], which is gradually moving OSCs closer to commercialization. However, poor material properties such as low charge carrier mobilities, low dielectric constants, and poor band offsets have led to the low PCE of OSCs relative to their silicon counterparts [1]. Hence, optimization of these parameters is essential for improving the performance of OSCs. Considerable attention has recently been focused on exploring strategies for the further optimization of the PCE, guided by a thorough understanding of the fundamental mechanisms that govern the photovoltaic performance of OSCs [7]. The following four processes distinguish BHJ OSCs from their inorganic counterparts: (i) photon absorption and exciton formation; (ii) exciton diffusion to the donor-acceptor (D-A) interface; (iii) exciton dissociation into free charge carriers at the D-A interface; and (iv) charge transport and

collection at their respective electrodes [8,9]. These processes should be efficient enough to achieve an enhanced PCE of BHJ OSCs.

One of the important parameters of BHJ OSCs is the open-circuit voltage V_{OC}, which is the voltage at which the net current flowing through the device is zero. It is established that in BHJ OSCs, V_{OC} depends on the energetic difference between the lowest unoccupied molecular orbital (LUMO) of the acceptor material ($E^{\mathrm{A}}_{\mathrm{LUMO}}$) and the highest occupied molecular orbital (HOMO) of the donor material ($E^{\mathrm{D}}_{\mathrm{HOMO}}$), called the donor-acceptor effective energy gap (E_{DA}) [10–14]. Until now, the most explored approach to increasing V_{OC} of BHJ OSCs has been to increase the energy of the LUMO of the fullerene acceptor material or decrease the energy of the HOMO of the donor material, or both [10–15]. Scharber and co-workers [10] empirically defined V_{OC} as:

$$qV_{OC} = E^{\mathrm{A}}_{\mathrm{LUMO}} - E^{\mathrm{D}}_{\mathrm{HOMO}} - \Delta E_{\mathrm{loss}} \tag{1}$$

where q is the elementary charge and ΔE_{loss} is an empirical value denoting the energy losses occurring in transporting the charge carriers to the electrodes [16–18].

The validity of Equation (1) has been established for a number of donor-acceptor (fullerene) blends with a voltage loss ΔE_{loss} ranging from $0.3-0.6$ eV [19,20]. The question that may be asked is: what are the possible causes of the voltage loss ΔE_{loss} and how can it be reduced? The origin of ΔE_{loss} is still being debated, with several possible mechanisms such as bimolecular recombination, coulombic interactions, energetic disorder, etc., [12,16–18,21,22]. An important loss mechanism in BHJ OSCs is the bimolecular recombination of free charge carriers with its rate R given by [23,24]:

$$R = \gamma np \tag{2}$$

where $\gamma = \gamma_{pre}\frac{q}{\varepsilon_0\varepsilon_r}(\mu_e + \mu_h)$ is the bimolecular recombination coefficient ($\mathrm{m^3s^{-1}}$): γ_{pre} is the dimensionless reduction prefactor, ε_0 is the permittivity of free space, ε_r is the dielectric constant, and $\mu_e(\mu_h)$ is the electron (hole) mobility ($\mathrm{m^2/Vs}$) in the active organic layer.

By minimizing the nonradiative bimolecular recombination in BHJ OSCs [25], one can minimize the voltage loss and eventually increase V_{OC}. Recent studies [26,27] have shown that V_{OC} can be determined more accurately by measuring the bimolecular recombination rate. These studies have also considered the influence of light intensity on V_{OC} by varying the carrier concentration due to photoexcitation. Lange et al. [28] studied the dependence of V_{OC} on the charge carrier concentration in polymer:fullerene blends using bias amplified charge extraction (BACE) measurements. In addition, as stated above, the energy loss also occurs due to the energetic disorder, which reduces the V_{OC}. A few recent studies have shown the effect of energetic disorder on V_{OC} using a Gaussian density of states (DOS) [29–31]. Garcia et al. [29] developed a model to predict the V_{OC} values by introducing DOS distributions of the HOMO in donor and the LUMO in acceptor materials. In their study, the energetic disorder is modeled by the Gaussian DOS with the mean energy equal to $E^{\mathrm{A}}_{\mathrm{LUMO}}$ and standard deviation σ_e for the acceptor material and corresponding $E^{\mathrm{D}}_{\mathrm{HOMO}}$ and σ_h for the donor material. In other studies [16,25,32–36], the role of energetics with respect to charge carrier dynamics and coulombic interactions have been analyzed. Credgington and Durrant [32] studied the dependence of V_{OC} on the generation and recombination dynamics; they studied the dependence of V_{OC} on the charge carrier concentration and carrier recombination lifetime. Vandewal et al. [25,33–35] derived a relationship between V_{OC} and the energy of the charge transfer (CT) exciton state E_{CT} by incorporating the energetic disorders. However, other works [16,36] have derived different expressions relating V_{OC} and E_{CT} in OSCs which exclude the influence of energetic disorder.

Despite numerous attempts to study V_{OC} and the associated energetic loss mechanisms in BHJ OSCs, there appears to be few attempts being made to understand whether it depends on the concentration of photoexcited charge carriers in the donor and acceptor materials. This may be due to the fact that as the two materials, donor and acceptor, are blended together in a BHJ structure, they cannot be separately excited experimentally. However, in order to understand the contributions

of photoexcitation of donor and acceptor materials to the performance of a BHJ OSC, one may seek to assess the performance considering the two cases separately: (1) when absorption and photoexcitation occur only in the donor and (2) when these occur only in the acceptor. Such a study can only be carried out theoretically, as presented here. When an exciton is excited in the donor in a BHJ OSC, its electron can be transferred from the donor LUMO to the acceptor LUMO at the D-A interface because the acceptor LUMO lies at a lower energy (see Figure 1a). In this process, an exciton becomes a CT exciton as its electron is transferred to the acceptor and its hole remains in the donor, as shown in Figure 1c. Likewise, when an exciton is excited in the acceptor, its hole can be transferred from the acceptor HOMO to the donor HOMO, being at a lower hole energy (see Figure 1b), which also creates a CT exciton with an electron in the acceptor LUMO and a hole in the donor HOMO, as shown in Figure 1c.

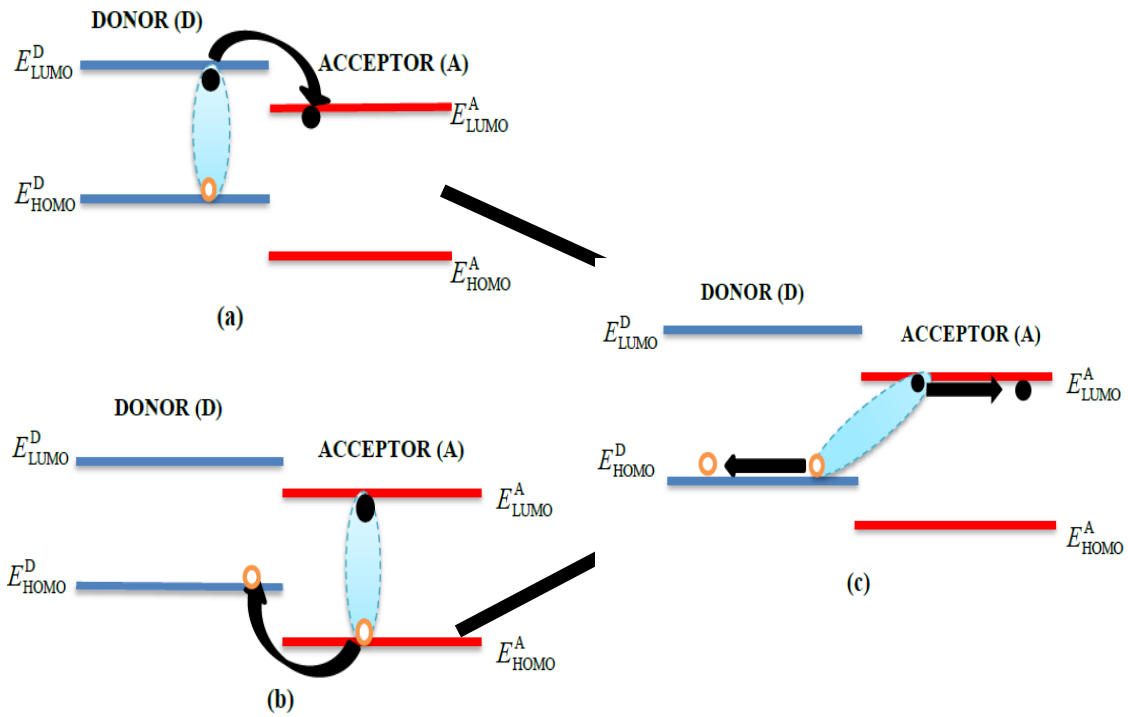

Figure 1. Schematic representations of (**a**) the photoexcitation of the donor and the transfer of an electron to the acceptor at the interface; (**b**) the photoexcitation of the acceptor and the transfer of a hole to the donor at the interface; and (**c**) the formation of charge transfer excitons (CT) through both (a,b) processes in bulk heterojunction (BHJ) organic solar cells (OSCs).

This has prompted several researchers to investigate the above two processes in more detail [37–46]. Recently, two different external quantum efficiencies (EQE) due to different donor and acceptor absorption bands have been reported [37]. The difference in the absorption bands can be attributed to the difference in the energy levels involved. The times of transfer of electrons from the donor LUMO to the acceptor LUMO and that of holes from the HOMO of the acceptor to the HOMO of the donor have been measured [38,39] and have been found to be different; the hole transfer was found to be faster than the electron transfer. This may be expected to lead to generating different concentrations n and p of electrons and holes. Different charge generations by exciting the donor and acceptor individually have also been reported in some donor-acceptor combinations [40], and different internal quantum efficiencies (IQE) have also been observed [41]. Some studies have demonstrated that BHJ OSCs based on thienothiophene-substituted diketopyrrolopyrrole (DPP) polymers (PDPP2TT-T) possess an EQE of 0.63–0.78 within the wavelength range of acceptor-fullerene absorption (400–650 nm), whereas a lower EQE of 0.35–0.50 is achieved within the range of donor-polymer absorption (650–900 nm) [41,42]. Such a difference may not be attributed to a difference in absorption of

photons in the different materials, but may be due to the difference in charge generation. In another study, Baulin et al. [43] compared the dynamics of CT states generated through electron-transfer and hole-transfer exciton-dissociation pathways in three BHJ OSCs, and they found that the dynamics of CT state recombination are very similar for the two charge-generation processes, implying that the nature of the generated CT states is independent of the pathways of CT formation. They did, however, observe that the generation of CT states and free charge carriers greatly depends on the actual LUMO energy offset $\Delta E_{\mathrm{LUMO}} = E^{\mathrm{D}}_{\mathrm{LUMO}} - E^{\mathrm{A}}_{\mathrm{LUMO}}$ (electron transfer) and the HOMO energy offset $\Delta E_{\mathrm{HOMO}} = E^{\mathrm{D}}_{\mathrm{HOMO}} - E^{\mathrm{A}}_{\mathrm{HOMO}}$ (hole transfer) of the blended system [44]. These energy offsets are independent of the pathway of the formation of CT excitons. Singh et al. [45,46] recently studied the contribution of exciton generation in the donor and acceptor materials and its dissociation to the performance of BHJ OSCs. They found that the absorption and dissociation rates as well as exciton diffusion lengths are comparable whether excitons are generated in the donor or acceptor.

In this paper, we investigate in detail the difference in the open circuit voltage from the photoexcited donor and photoexcited acceptor separately in the following seven different polymer:fullerene blends: poly[2-methoxy-5-(3′,7′-dimethyloctyloxy)-1,4-phenylenevinylene] (MDMO-PPV), regioregular poly(3-hexylthiophene) (P3HT), poly[N-9′-heptadecanyl-2,7-carbazole-alt-5,5-(4′,7′-di-2-thienyl-2′,1′,3′-benzothiadiazole)] (PCDTBT), poly[2-(3,7-dimethoxyoctyloxy)-5-methoxy-1,4-phenylene vinylene] (OC_1C_{10}-PPV), poly[4,8-bis[(2-ethylhexyl)oxy]benzo[1,2-b:4,5-b′]dithiophene-2,6-diyl][3-fluoro-2-[(2-ethylhexyl)carbonyl]thieno[3,4-b]thiophenediyl] (PTB7), mono-DPP, and bis-DPP blended with different derivatives of methano-fullerene[6,6]-phenyl C_{61},-butyric acid methyl ester (PCBM). We derived two different expressions for V_{OC} in BHJ OSCs. The first expression, which is a result of photoexcitation of the donor, depends primarily on the energetic difference between the hole quasi-Fermi level (E^h_F) and the HOMO of the donor material $(E^h_F - E^{\mathrm{D}}_{\mathrm{HOMO}})$ and the electron concentration n. The second expression, which is a result of photoexcitation of the acceptor, depends primarily on the energetic difference between the LUMO and the electron quasi-Fermi level (E^e_F) of the acceptor material $(E^{\mathrm{A}}_{\mathrm{LUMO}} - E^e_F)$ and the hole concentration p. Thus, the two open circuit voltages calculated in each selected D-A blend are presented here and their influences on the performance of BHJ OSCs are discussed. Following this, the simultaneous photoexcitation of both the donor and acceptor materials is also considered and the corresponding V_{OC}, which is different from the above two, is derived, and the calculated V_{OC}s are compared with their corresponding measured values and a reasonably good agreement is found between them.

2. Theoretical Formalism

Under no illumination condition of equilibrium, assuming the condition of the open circuit voltage in a BHJ OSC, the electron and hole current densities are assumed to be independently zero, and under this condition the quasi-Fermi levels in the donor and acceptor materials are iso-energetic at energy E_F throughout the device. Once such a BHJ OSC is illuminated, charge carriers are continuously generated in the active layer. As the concentration of charge carriers increases, the quasi-Fermi level E_F splits into the hole and electron quasi-Fermi levels located, respectively, at energies E^h_F in the donor material and at E^e_F in the acceptor, as shown in Figure 2.

Under the condition of illumination, V_{OC} in any BHJ OSC is given by [47]:

$$qV_{OC} = E^e_F - E^h_F \tag{3}$$

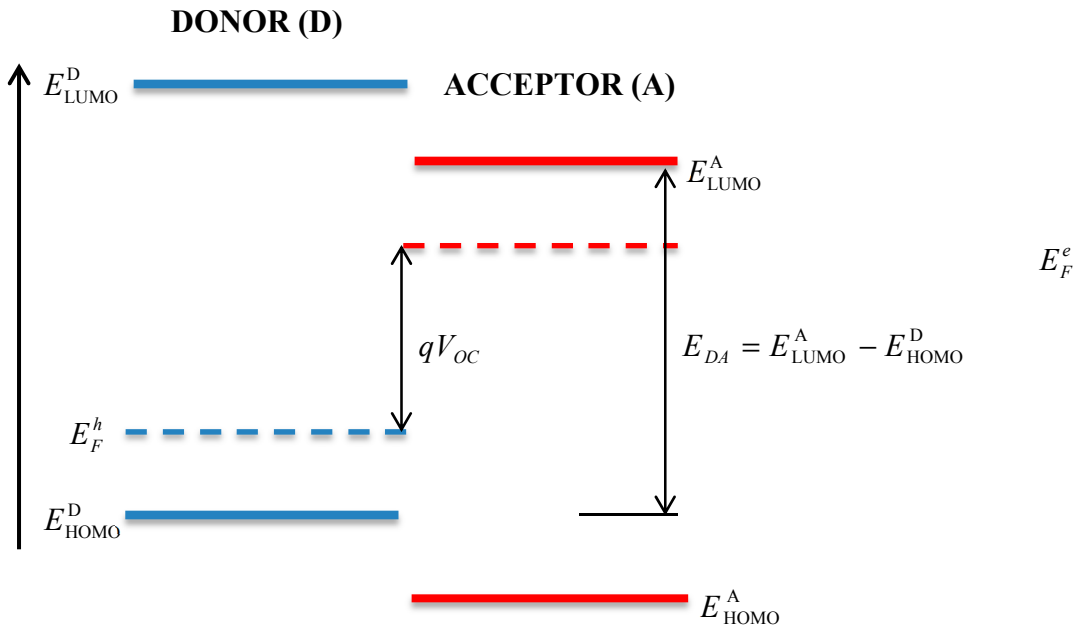

Figure 2. Schematic representation of the different energy levels, quasi-Fermi energy levels, and V_{OC} in a BHJ OSC with a donor-acceptor blend under the open circuit condition.

The Fermi energies E_F^e and E_F^h may be expected to be different for excitations of the donor and acceptor individually. Although the difference may not be expected to be significant, this may lead to two different values of V_{OC} according to Equation (3).

2.1. Photoexcitation of the Donor

We consider the photoexcitation of only the donor material here, where an excited exciton at the D-A interface forms a CT exciton by transferring its electron to the acceptor's LUMO, being at a lower energy [48]. The electron concentration (n) in the LUMO of the fullerene-acceptor material and the hole concentration (p) in the HOMO of the polymer-donor material are, respectively, given by the Boltzmann distribution as [49]:

$$n = N_C \exp[(E_F^e - E^{A}_{LUMO})/k_B T] \tag{4}$$

$$p = N_V \exp[(E^{D}_{HOMO} - E_F^h)/k_B T] \tag{5}$$

where $N_C(N_V)$ (m^{-3}) is the effective density of states for the LUMO (HOMO) of the acceptor (donor) material, T is the temperature, and k_B is the Boltzmann constant.

Under the conditions of V_{OC} and bimolecular recombination, the generation rate of photoexcited electron and hole pairs G is equal to the bimolecular recombination rate given in Equation (2), which gives:

$$G = R = \gamma np \tag{6}$$

Assuming a non-optimized BHJ OSC with unbalanced charge carrier mobilities $(\mu_e \neq \mu_h)$, we assume that $n \neq p$ [39,40], and then divide Equation (6) by n^2 to obtain:

$$\frac{p}{n} = \frac{G}{\gamma n^2} \tag{7}$$

Dividing Equation (5) by Equation (4) and using it in Equation (7) gives:

$$\frac{G}{\gamma n^2} = \frac{N_V}{N_C} \exp[\frac{1}{k_B T}(E^{\mathrm{D}}_{\mathrm{HOMO}} + E^{\mathrm{A}}_{\mathrm{LUMO}} - E^h_F - E^e_F)] \tag{8}$$

Substituting $E^{\mathrm{A}}_{\mathrm{LUMO}} = E^{\mathrm{D}}_{\mathrm{HOMO}} + E_{DA}$ into Equation (8) and using Equation (3), we get:

$$k_B T \ln \frac{N_C G}{N_V \gamma n^2} = (2E^{\mathrm{D}}_{\mathrm{HOMO}} - 2E^h_F - qV_{OC} + E_{DA}) \tag{9}$$

Assuming $N_C = N_V$ [38,41], and rearranging Equation (9), we obtain V_{OC} related to the excitation of donor only as:

$$V^D_{OC} = \frac{1}{q}(E_{DA} - A + 2k_B T \ln n) \tag{10}$$

where:

$$A = 2(E^h_F - E^{\mathrm{D}}_{\mathrm{HOMO}}) + k_B T \ln(G/\gamma) \tag{11}$$

2.2. Photoexcitation of the Acceptor

Next, we consider the photoexcitation of only the acceptor material, where the excited exciton at the D-A interface forms a CT exciton by transferring its hole to the donor's HOMO, being at a lower energy [48]. This gives a different open circuit voltage, which is derived as follows.

Here, we divide both sides of Equation (6) by p^2 to obtain:

$$\frac{n}{p} = \frac{G}{\gamma p^2} \tag{12}$$

Dividing Equation (4) by Equation (5) and using it in Equation (12) gives:

$$\frac{G}{\gamma p^2} = \frac{N_C}{N_V} \exp[\frac{1}{k_B T}(E^e_F - E^{\mathrm{D}}_{\mathrm{HOMO}} - E^{\mathrm{A}}_{\mathrm{LUMO}} + E^h_F)] \tag{13}$$

Substituting $E^{\mathrm{D}}_{\mathrm{HOMO}} = E^{\mathrm{A}}_{\mathrm{LUMO}} - E_{DA}$ into Equation (13) and using Equation (3), we get:

$$k_B T \ln \frac{N_C G}{N_V \gamma p^2} = (2E^e_F - 2E^{\mathrm{A}}_{\mathrm{LUMO}} - qV_{OC} + E_{DA}) \tag{14}$$

Assuming $N_C = N_V$ [38,41] and rearranging Equation (14), we obtain V_{OC} for this case as:

$$V^A_{OC} = \frac{1}{q}(E_{DA} - B + 2k_B T \ln p) \tag{15}$$

where:

$$B = 2(E^{\mathrm{A}}_{\mathrm{LUMO}} - E^e_F) + k_B T \ln(G/\gamma) \tag{16}$$

We have thus derived two different expressions for the V_{OC}; the first one in Equation (10) is obtained when the donor material is excited and the second in Equation (15) is obtained when the acceptor is excited.

2.3. Simultaneous Photoexcitation of the Donor and Acceptor

The theoretical developments presented in Sections 2.1 and 2.2, where only the donor or acceptor is excited, are mostly applicable in layered structures of donor and acceptor organic solar cells. However, in a BHJ OSC where the donor and acceptor are blended together in the active layer, both the donor and acceptor may be excited simultaneously. In this case, we obtain a different V_{OC} as follows.

Multiplying Equations (4) and (5), we obtain:

$$np = N_C N_V \exp[(E_F^e - E_F^h + E_{\mathrm{HOMO}}^{\mathrm{D}} - E_{\mathrm{LUMO}}^{\mathrm{A}})/k_B T] \tag{17}$$

Substituting $-E_{DA} = E_{\mathrm{HOMO}}^{\mathrm{D}} - E_{\mathrm{LUMO}}^{\mathrm{A}}$ and using Equation (3) in Equation (17) we thus get:

$$V_{OC}^{DA} = \frac{1}{q}[E_{DA} - C + 2k_B T \ln \sqrt{(np)}] \tag{18}$$

where:

$$C = k_B T \ln N_C N_V \tag{19}$$

It may be noted that, unlike V_{OC}s obtained in Equations (10) and (15), which depend on the electron (n) and hole (p) concentrations, respectively, Equation (18) depends on both n and p. The dependence of V_{OC} in Equation (18) on $\sqrt{np}$ is presented mainly to compare it with the results derived in Equations (10) and (15).

3. Results

For calculating the V_{OC} using Equations (10), (15), and (18), we require some material-dependent input parameters. For this, as stated above, we chose seven donor-acceptor blends with known input parameters available in the literature, as listed in Table 1.

Table 1. List of input parameters required for calculating V_{OC} from Equations (10), (15), and (18): $E_{DA}/q = (E_{\mathrm{LUMO}}^{\mathrm{A}} - E_{\mathrm{HOMO}}^{\mathrm{D}})/q$, generation rate of bound polaron pairs (G) and bimolecular recombination coefficient (γ), electron (hole) mobility $\mu_e(\mu_h)$, and dielectric constant ε_r of each donor-acceptor (D-A) blend.

Active Layer Blend	$\frac{E_{DA}}{q}$ (V)	G (10^{27} m^{-3}s^{-1})	γ (10^{-17} m^{3}s^{-1})	μ_e (m^{2}V^{-1}s^{-1})	μ_h (m^{2}V^{-1}s^{-1})	ε_r
MDMO-PPV:PC$_{61}$BM	1.30 [1]	2.7 [8]	5.73	2×10^{-7} [8]	2×10^{-8} [8]	3.4 [8]
P3HT:PC$_{60}$BM	1.00 [2]	6.25 [2]	7.08	1×10^{-7} [2]	1×10^{-8} [2]	3.4 [2]
PCDTBT:PC$_{71}$BM	1.20 [3]	1.0 [9]	0.1	2.9×10^{-7} [9]	3.0×10^{-9} [9]	3.4 [9]
OC$_1$C$_{10}$-PPV:PC$_{61}$BM	1.30 [4]	2.7 [10]	7.30	2.5×10^{-7} [10]	3.0×10^{-8} [10]	3.4 [10]
PTB7:PC$_{71}$BM	1.09 [5]	10 [11]	5.91	1×10^{-7} [11]	2.0×10^{-8} [11]	3.5 [11]
mono-DPP:PC$_{71}$BM	1.16 [6]	4.99 [13]	5.3	1×10^{-7} [12]	2.0×10^{-9} [12]	4.0 [12]
bis-DPP:PC$_{71}$BM	1.20 [7]	4.12 [14]	2.6	1.5×10^{-7} [12]	3.4×10^{-8} [12]	4.0 [12]

[1] [50]; [2] [51]; [3] [52]; [4] [53]; [5] [54]; [6] [55]; [7] [56]; [8] [57]; [9] [58]; [10] [59]; [11] [60]; [12] [61].

The values of γ for PCDTBT:PC$_{71}$BM [58], mono-DPP:PC$_{71}$BM [61], and bis-DPP:PC$_{71}$BM [61] are taken from the literature, and those of the remaining four blends, MDMO-PPV:PC$_{61}$BM P3HT:PC$_{60}$BM, OC$_1$C$_{10}$-PPV:PC$_{61}$BM, and PTB7:PC$_{71}$BM, are calculated using the bimolecular recombination coefficient equation described in the text. In addition, we need the values of $(E_F^h - E_{\mathrm{HOMO}}^{\mathrm{D}})$ and $(E_{\mathrm{LUMO}}^{\mathrm{A}} - E_F^e)$, as well as the carrier concentrations n and p in each blend to calculate V_{OC} from Equations (10), (15), and (18), which are also listed in Tables 2 and 3. However, it may be noted that both n and p are only available for PTB7:PC$_{71}$BM [62] as given in Tables 2 and 3. In mono-DPP:PC$_{71}$BM and bis-DPP:PC$_{71}$BM, only the electron concentration n is known in the literature [63]. Consequently, to find the hole concentration p in these two blends, we used Equation (7) and calculated p; these n and p thus obtained are listed in Tables 2 and 3. We first used the n and p values determined above for PTB7:PC$_{71}$BM, mono-DPP:PC$_{71}$BM, and bis-DPP:PC$_{71}$BM in Equations (4) and (5), and calculated their energetic distances $(E_{\mathrm{LUMO}}^{\mathrm{A}} - E_F^e)$ and $(E_F^h - E_{\mathrm{HOMO}}^{\mathrm{D}})$, respectively, at 300 K by assuming the effective density of states $N_C = N_V = 1 \times 10^{25}$ m^{-3} in each blend.

Table 2. The calculated values of $(E_F^h - E_{\mathrm{HOMO}}^{\mathrm{D}})/q$ and electron concentration n used in calculating the open circuit voltage V_{OC}^D from Equation (10), the calculated voltage offset $(E_{DA}/q - V_{OC}^D)$ for comparison with other known results, and the corresponding measured open circuit voltage $V_{OC}^{\mathrm{meas.}}$.

Active Layer Blend	$(E_F^h - E_{\mathrm{HOMO}}^{\mathrm{D}})/q$ (V)	n (m^{-3})	V_{OC}^D (V)	$(E_{DA}/q - V_{OC}^D)$ (V)	$V_{OC}^{\mathrm{meas.}}$ (V)
MDMO-PPV:PC$_{61}$BM	0.20	1.80×10^{22}	0.95	0.35	0.83 [64]
P3HT:PC$_{60}$BM	0.26	1.80×10^{22}	0.51	0.49	0.63 [51]
PCDTBT:PC$_{71}$BM	0.22	1.80×10^{22}	0.73	0.47	0.85 [65]
OC$_1$C$_{10}$-PPV:PC$_{61}$BM	0.20	1.80×10^{22}	0.96	0.34	0.85 [59]
PTB7:PC$_{71}$BM	0.18	1.90×10^{22}	0.75	0.34	0.75 [54]
mono-DPP:PC$_{71}$BM	0.20	2.50×10^{22}	0.81	0.35	0.78 [61]
bis-DPP:PC$_{71}$BM	0.17	1.00×10^{22}	0.85	0.35	0.52 [61]

Table 3. The calculated values of $(E_{\mathrm{LUMO}}^{\mathrm{A}} - E_F^e)/q$ and hole concentration p used in calculating open-circuit voltage V_{OC}^A from Equation (15), the calculated voltage offset $(E_{DA}/q - V_{OC}^A)$, and the corresponding measured open circuit voltage $V_{OC}^{\mathrm{meas.}}$.

Active Layer Blend	$(E_{\mathrm{LUMO}}^{\mathrm{A}} - E_F^e)/q$ (V)	p (m^{-3})	V_{OC}^A (V)	$(E_{DA}/q - V_{OC}^A)$ (V)	$V_{OC}^{\mathrm{meas.}}$ (V)
MDMO-PPV:PCBM	0.18	0.95×10^{22}	0.93	0.37	0.83 [64]
P3HT:PC$_{60}$BM	0.24	0.95×10^{22}	0.52	0.48	0.63 [51]
PCDTBT:PC$_{71}$BM	0.20	0.95×10^{22}	0.73	0.47	0.85 [65]
OC$_1$C$_{10}$-PPV:PC$_{61}$BM	0.19	0.95×10^{22}	0.94	0.36	0.85 [59]
PTB7:PC$_{71}$BM	0.16	0.89×10^{22}	0.75	0.34	0.75 [54]
mono-DPP:PC$_{71}$BM	0.16	0.38×10^{22}	0.79	0.37	0.78 [61]
bis-DPP:PC$_{71}$BM	0.18	1.58×10^{22}	0.85	0.35	0.52 [61]

For the other four blends considered here, MDMO-PPV:PC$_{61}$BM, P3HT:PC$_{60}$BM, PCDTBT:PC$_{71}$BM, and OC$_1$C$_{10}$-PPV:PC$_{61}$BM, the n and p concentrations are not known. As the n and p concentrations in all the three materials are of the order of 10^{22} m^{-3} (see Tables 2 and 3), we used the average values of n, which is 1.8×10^{22} m^{-3}, and p, which is 0.95×10^{22} m^{-3}, for PTB7:PC$_{71}$BM, mono-DPP:PC$_{71}$BM, and bis-DPP:PC$_{71}$BM, and calculated the energetic distances $(E_F^h - E_{\mathrm{HOMO}}^{\mathrm{D}})$ and $(E_{\mathrm{LUMO}}^{\mathrm{A}} - E_F^e)$ for the other four blends (see Tables 2 and 3). That is to say, using Equations (4) and (5) with $N_C = N_V = 2.5 \times 10^{25}$ m^{-3} known for MDMO-PPV:PC$_{61}$BM [17,57], $N_C = N_V = 2 \times 10^{26}$ m^{-3} for P3HT:PC$_{60}$BM [1], $N_C = N_V = 5 \times 10^{25}$ m^{-3} for PCDTBT:PC$_{71}$BM [52], and $N_C = N_V = 2.5 \times 10^{25}$ m^{-3} for OC$_1$C$_{10}$-PPV:PC$_{61}$BM [1,59], in addition to the corresponding average charge carrier concentrations $n = 1.8 \times 10^{22}$ m^{-3} and $p = 0.95 \times 10^{22}$ m^{-3}, we calculated $(E_{\mathrm{LUMO}}^{\mathrm{A}} - E_F^e)$ and $(E_F^h - E_{\mathrm{HOMO}}^{\mathrm{D}})$, respectively, in the other four blends.

Using these parameters in Equations (10) and (15), the V_{OC} is calculated in all seven blends for the photoexcitation of the donor and acceptor as given in Tables 2 and 3, respectively. The calculated values of V_{OC} from Equation (10) when the donor is excited in most selected materials are somewhat comparable with those calculated from Equation (15) when the acceptor is excited, as also shown in Figure 3. In addition, considering the case of simultaneous photoexcitation of donor and acceptor materials, the open circuit voltage in each blend is calculated from Equation (18) as given in Table 4. All the three V_{OC}s obtained from the asynchronous and simultaneous photoexcitations of donor and acceptor are found to be comparable and agree well with the corresponding measured values [51,54,59,61,64,65].

The open circuit voltages V_{OC}s calculated from Equations (10) and (15) are plotted as a function of the effective band gap E_{DA}/q as shown in Figure 3, which illustrates that V_{OC} calculated from Equation (10) is slightly higher than that from Equation (15).

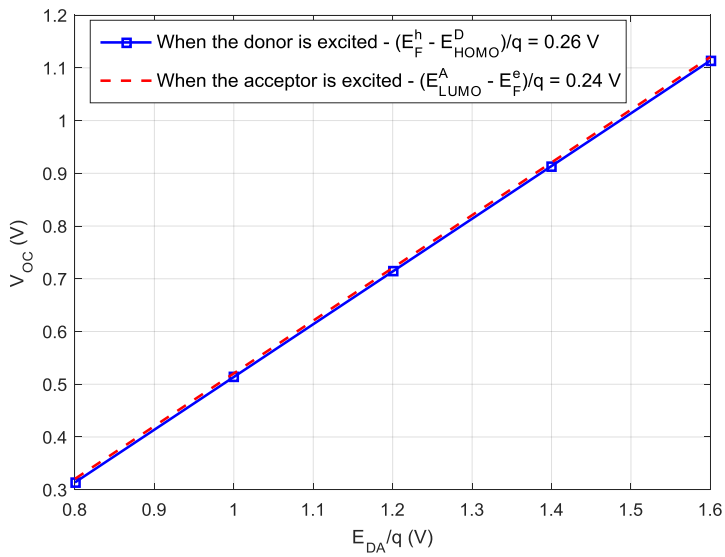

Figure 3. Open circuit voltage V_{OC} plotted as a function of effective band gap E_{DA}/q for non-optimized P3HT:PC_{60}BM with large photocarrier mobility mismatch ($\mu_e \neq \mu_h$), at energetic distances $(E_F^h - E_{\mathrm{HOMO}}^{\mathrm{D}})/q$ = 0.26 V with n = 1.80 × 10^{22} m^{-3} and $(E_{\mathrm{LUMO}}^{\mathrm{A}} - E_F^e)/q$ = 0.24 V with p = 0.95 × 10^{22} m^{-3} in the donor and acceptor materials, respectively.

Table 4. The calculated values of open circuit voltage V_{OC}^{DA} from Equation (18) using the n and p values listed in Tables 2 and 3, respectively, voltage offset $(E_{DA}/q - V_{OC}^{DA})$ upon simultaneous excitation of both the donor and acceptor materials, and the corresponding measured open circuit voltage $V_{OC}^{\mathrm{meas.}}$.

Active Layer Blend	V_{OC}^{DA} (V)	$(E_{DA}/q - V_{OC}^{DA})$ (V)	$V_{OC}^{\mathrm{meas.}}$ (V)
MDMO-PPV:PC_{61}BM	0.91	0.39	0.83 [64]
P3HT:PC_{60}BM	0.50	0.50	0.63 [51]
PCDTBT:PC_{71}BM	0.77	0.43	0.85 [65]
OC_1C_{10}-PPV:PC_{61}BM	0.91	0.39	0.85 [59]
PTB7:PC_{71}BM	0.74	0.35	0.75 [54]
mono-DPP:PC_{71}BM	0.79	0.37	0.78 [61]
bis-DPP:PC_{71}BM	0.85	0.35	0.52 [61]

Finally, as stated previously, in a BHJ OSC the donor and acceptor materials are blended together. Consequently, both the donor and acceptor are excited simultaneously, resulting in one open circuit voltage as derived in Equation (18), which is used to calculate the V_{OC}^{DA} for simultaneous photoexcitations of both the donor and acceptor in each of the selected blends, as listed in Table 4. The measured values of open circuit voltage $V_{OC}^{\mathrm{meas.}}$ are also given in Table 4 for comparison.

4. Discussions

A comprehensive study of the open circuit voltage in BHJ OSCs has been carried out. Three different expressions for V_{OC} are derived; the first in Equation (10) is obtained when the donor material in a BHJ OSC is excited, the second in Equation (15) is obtained when the acceptor material is excited, and the third in Equation (18) is obtained when both the donor and acceptor materials are excited simultaneously. As stated previously, when the photoexcitation occurs in the donor, an electron is transferred from the LUMO of the donor to the LUMO of the acceptor, and conversely, when photoexcitation occurs in the acceptor, a hole is transferred from the HOMO of the acceptor to the HOMO of the donor [48]. The photoexcitation of the donor and acceptor individually produces comparable V_{OC} values from Equations (10) and (15), as shown in Figure 3. Moreover, according to Figure 3, the linear correlation between V_{OC} and E_{DA}/q agrees well with

previous studies [20,30,32,33,64]. The third open circuit voltage V_{OC}^{DA} calculated in Equation (18) from the simultaneous excitations of both the donor and acceptor, as given in Table 4, is also comparable with the other two V_{OC}s. All three V_{OC}s thus derived produce comparable results and agree reasonably well with the experimental values (see Tables 2–4). However, the calculated V_{OC} values in Tables 2–4 are obtained from slightly different energetic parameters; as a result, we obtained three different sets of V_{OC}s for the photoexcitation of the donor, photoexcitation of the acceptor, and simultaneous photoexcitation of both. However, experimentally, there is only one set of measured values of V_{OC} to compare the theoretical results with. As a result, the calculated range of V_{OC} for the materials considered here is 0.50–0.96 V, which is slightly different from the range of experimental values (0.52–0.85 V). Thus, as stated above, this discrepancy may be attributed to the different energies $(E_F^h - E_{\mathrm{HOMO}}^{\mathrm{D}})/q$ used in the calculation of V_{OC} from Equations (10), (15), and (18).

In addition, the two V_{OC}s in Equations (10) and (15) depend linearly on $\ln n$ and $\ln p$, respectively, and this agrees well with previously measured results [28,63]. This also holds for V_{OC} derived from Equation (18), which depends on $\ln(\sqrt{np})$. By setting $n = p$ in Equations (10), (15), and (18), we found that all three V_{OC}s increase linearly with $\ln n$ and have the same slope equal to $\frac{k_B T}{q}/\log(\exp(1)) \approx 2.3 \times 2k_B T/q \approx 119$ mV. This implies that the materials with higher photo-generated charge carrier concentration will have higher V_{OC} in comparison with materials with lower carrier concentration.

It is also worth noting that the dependence of V_{OC} on the incident light intensity has been studied [17,24]. Substituting $np = \frac{G}{\gamma} \propto I_{abs} = I_o[1 - \exp(-\alpha t)]$ into Equation (18), where I_{abs} is the absorbed light intensity, I_0 is the incident light intensity, α is the absorption coefficient, and t is the thickness of the active layer, we get:

$$V_{OC}^{DA} = \frac{1}{q}[E_{DA} + k_B T \ln I_0 + \text{constant}] \tag{20}$$

The V_{OC} in Equation (20) depends linearly on $\ln I_0$ with a slope of $\frac{k_B T}{q}$, which agrees perfectly well with the plotted V_{OC} as a function of $\ln I_0$ in [17,24].

Orlowski et al. [66] used the energetics of quasi-Fermi levels to study V_{OC} in a heterojunction solar cell. They found that for a particular donor (p-type)-acceptor (n-type) heterojunction, the electron concentration (n) in the conduction band (LUMO) of the acceptor and the hole concentration (p) in the valence band (HOMO) of the donor, coupled with their respective quasi-Fermi levels, can create open circuit voltages like two independent cells. This agrees very well with our concept of deriving two different V_{OC}s in Equations (10) and (15), although both the expressions produce similar results.

Furthermore, we find that the V_{OC}^{D} lies 0.34–0.49 V below the E_{DA}/q in column 5 of Table 2 when the donor is excited, comparable to 0.34–0.48 V below the E_{DA}/q in column 5 of Table 3 when the acceptor is excited. This implies that both the donor and acceptor photoexcitations can contribute to the achievable open circuit voltage as well as the photovoltaic performance of BHJ OSCs; this agrees with our earlier results [45]. The voltage offsets $(E_{DA}/q - V_{OC}^{j})$ (where $j = D,\ A\ or\ DA$) of the various blends listed in Tables 2–4, ranging from 0.34–0.50 V, agree well with the experimental values measured at room temperature in the range of 0.25–0.48 V for small molecule OSCs [67], 0.32 V for polymer:fullerene solar cells of indacenoedithiophene (IDT) polymer [68], 0.34–0.44 V for a range of donor-acceptor blends [69], 0.38 V for OC_1C_{10}-PPV:PCBM solar cells [12], and 0.30–0.60 V for BHJ OSCs [20]. Other low voltage offsets $(E_{DA}/q - V_{OC}^{j})$ that have been reported recently are 0.25 V for an evaporated bilayer OSC [70], 0.23 V and 0.26 V for diketopyrrolopyrrole-thieno[2,3-f]benzofuran (DTD):PC_{60}BM and DTD:naphthalene diimide acceptor-polymer (N2200) systems, respectively [71], and 0.34–0.40 V for BHJ OSCs [72], with which our calculated values also somewhat agree in the range.

Overall, it may be deduced from our results that separate and simultaneous photoexcitations of the donor and acceptor produce comparable V_{OC}s, and the highest loss in V_{OC} is found to be contributed by the energetics of the donor and acceptor materials. Therefore, to achieve a high V_{OC}, it is necessary to choose higher efficiency polymer-donor and acceptor materials, as well as control

the donor and acceptor material energetics, which may lead to improvements in the PCEs of BHJ OSCs [32].

5. Conclusions

In summary, we have derived two different expressions for the calculation of the V_{OC} in BHJ OSCs; one is used when the exciton is excited in the donor material and the other is employed when the exciton is excited in the acceptor material. We have also derived an expression for V_{OC} when both the donor and acceptor materials are excited simultaneously, and its calculated values agree better with their measured values. All three V_{OC}s obtained from separate and simultaneous excitations are found to be comparable, implying that the contributions of both donor and acceptor photoexcitations are comparable in BHJ OSCs. Also, it is found that materials that generate higher photo-generated charge carrier concentrations and have lower energetic distances of $(E_F^h - E_{\mathrm{HOMO}}^{\mathrm{D}})$ or $(E_{\mathrm{LUMO}}^{\mathrm{A}} - E_F^e)$ may lead to higher V_{OC}. Invention and application of such materials in the fabrication of BHJ OSCs may lead to higher V_{OC}s and hence enhanced PCEs.

Author Contributions: Both the authors have contributed to the publication of this paper. Douglas Yeboah carried out all the calculations. With the guidance from Jai Singh, the paper was initially drafted by Yeboah and then was finalized by them together.

Conflicts of Interest: The authors declare no conflict of interest.

References

1. Inche Ibrahim, M.L.; Ahmad, Z.; Sulaiman, K.; Muniandy, S.V. Combined influence of carrier mobility and dielectric constant on the performance of organic bulk heterojunction solar cells. *AIP Adv.* **2014**, *4*, 057133. [CrossRef]
2. Zhong, Y.; Tada, A.; Izawa, S.; Hashimoto, K.; Tajima, K. Enhancement of V_{OC} without loss of J_{SC} in organic solar cells by modification of donor/acceptor interfaces. *Adv. Energy Mater.* **2014**, *4*, 1301332. [CrossRef]
3. Chen, C.-C.; Chang, W.-H.; Yoshimura, K.; Ohya, K.; You, J.; Gao, J.; Hong, Z.; Yang, Y. An efficient triple-junction polymer solar cell having a power conversion efficiency exceeding 11%. *Adv. Mater.* **2014**, *26*, 5670–5677. [CrossRef] [PubMed]
4. Zhao, J.; Li, Y.; Yang, G.; Jiang, K.; Lin, H.; Ade, H.; Ma, W.; Yan, H. Efficient organic solar cells processed from hydrocarbon solvents. *Nat. Energy* **2016**, *1*, 15027. [CrossRef]
5. Zhang, S.; Ye, L.; Hou, J. Breaking the 10% efficiency barrier in organic photovoltaics: Morphology and device optimization of well-known PBDTTT polymers. *Adv. Energy Mater.* **2016**, *6*, 1502529. [CrossRef]
6. Gan, Q.; Bartoli, F.J.; Kafafi, Z.H. Plasmonic-enhanced organic photovoltaics: Breaking the 10% efficiency barrier. *Adv. Mater.* **2013**, *25*, 2385–2396. [CrossRef] [PubMed]
7. Deibel, C.; Wagenpfahl, A.; Dyakonov, V. Influence of charge carrier mobility on the performance of organic solar cells. *Phys. Status Solidi* **2008**, *2*, 175–177. [CrossRef]
8. Narayan, R.M.; Singh, J. Study of the mechanism and rate of exciton dissociation at the donor-acceptor interface in bulk-heterojunction organic solar cells. *J. Appl. Phys.* **2013**, *114*. [CrossRef]
9. Ompong, D.; Singh, J. Diffusion length and Langevin recombination of singlet and triplet excitons in organic heterojunction solar cells. *ChemPhysChem* **2015**, *16*, 1281–1285. [CrossRef] [PubMed]
10. Scharber, M.C.; Muhlbacher, D.; Koppe, M.; Denk, P.; Waldauf, C.; Heeger, A.J.; Brabec, C.J. Design rules for donors in bulk-heterojunction solar cells—Towards 10% energy-conversion efficiency. *Adv. Mater.* **2006**, *18*, 789–794. [CrossRef]
11. Kietzke, T.; Egbe, D.A.M.; Hörhold, H.-H.; Neher, D. Comparative study of M3EH−PPV-based bilayer photovoltaic devices. *Macromolecules* **2006**, *39*, 4018–4022. [CrossRef]
12. Mihailetchi, V.D.; Blom, P.W.M.; Hummelen, J.C.; Rispens, M.T. Cathode dependence of the open-circuit voltage of polymer:fullerene bulk heterojunction solar cells. *J. Appl. Phys.* **2003**, *94*, 6849–6854. [CrossRef]
13. Ross, R.B.; Cardona, C.M.; Guldi, D.M.; Sankaranarayanan, S.G.; Reese, M.O.; Kopidakis, N.; Peet, J.; Walker, B.; Bazan, G.C.; van Keuren, E.; et al. Endohedral fullerenes for organic photovoltaic devices. *Nat. Mater.* **2009**, *8*, 208–212. [CrossRef] [PubMed]

14. Lenes, M.; Wetzelaer, G.; Kooistra, F.B.; Veenstra, S.C.; Hummelen, J.C.; Blom, P.W.M. Fullerene bisadducts for enhanced open-circuit voltages and efficiencies in polymer solar cells. *Adv. Mater.* **2008**, *20*, 2116–2119. [CrossRef]
15. Fengling, Z.; Bijleveld, J.; Perzon, E.; Tvingstedt, K.; Barrau, S.; Inganäs, O.; Andersson, M.R. High photovoltage achieved in low band gap polymer solar cells by adjusting energy levels of a polymer with the LUMOs of fullerene derivatives. *J. Mater. Chem.* **2008**, *18*, 5468–5474. [CrossRef]
16. Rand, B.; Burk, D.; Forrest, S. Offset energies at organic semiconductor heterojunctions and their influence on the open-circuit voltage of thin-film solar cells. *Phys. Rev. B* **2007**, *75*, 115327. [CrossRef]
17. Koster, L.J.A.; Mihailetchi, V.D.; Ramaker, R.; Blom, P.W.M. Light intensity dependence of open-circuit voltage of polymer:fullerene solar cells. *Appl. Phys. Lett.* **2005**, *86*, 123509. [CrossRef]
18. Riede, M.; Mueller, T.; Tress, W.; Schueppel, R.; Leo, K. Small-molecule solar cells-status and perspectives. *Nanotechnology* **2008**, *19*, 424001. [CrossRef] [PubMed]
19. Brabec, C.J.; Cravino, A.; Meissner, D.; Sariciftci, N.S.; Fromherz, T.; Rispens, M.T.; Sanchez, L.; Hummelen, J.C. Origin of the open circuit voltage of plastic solar cells. *Adv. Funct. Mater.* **2001**, *11*, 374–380. [CrossRef]
20. Yang, Q.-D.; Li, H.-W.; Cheng, Y.; Guan, Z.; Liu, T.; Ng, T.-W.; Lee, C.-S.; Tsang, S.-W. Probing the energy level alignment and the correlation with open-circuit voltage in solution-processed polymeric bulk heterojunction photovoltaic devices. *ACS Appl. Mater. Interfaces* **2016**, *8*, 7283–7290. [CrossRef] [PubMed]
21. Cho, N.; Schlenker, C.W.; Knesting, K.M.; Koelsch, P.; Yip, H.-Y.; Ginger, D.S.; Jen, A.K.-Y. High dielectric constant side-chain polymers show reduced non-geminate recombination in heterojunction. *Adv. Energy Mater.* **2014**, *4*, 1301857. [CrossRef]
22. Chen, S.; Tsang, S.W.; Lai, T.H.; Reynolds, J.R.; So, F. Dielectric effect on the photovoltage loss in organic photovoltaic cells. *Adv. Mater.* **2014**, *26*, 6125–6131. [CrossRef] [PubMed]
23. Koster, L.J.A.; Mihailetchi, V.D.; Blom, P.W.M. Bimolecular recombination in polymer/fullerene bulk heterojunction solar cells. *Appl. Phys. Lett.* **2006**, *88*, 052104. [CrossRef]
24. Cowan, S.R.C.; Roy, A.; Heeger, A.J. Recombination in polymer-fullerene bulk heterojunction solar cells. *Phys. Rev. B* **2010**, *82*, 245207. [CrossRef]
25. Vandewal, K.; Tvingstedt, K.; Gadisa, A.; Inganas, O.; Manca, J.V. On the origin of the open-circuit voltage of polymer-fullerene solar cells. *Nat. Mater.* **2009**, *8*, 904–909. [CrossRef] [PubMed]
26. Shuttle, C.G.; O'Regan, B.; Ballantyne, A.M.; Nelson, J.; Bradley, D.D.C.; Durrant, J.R. Bimolecular recombination losses in polythiophene: Fullerene solar cells. *Phys. Rev. B* **2008**, *78*, 113201. [CrossRef]
27. Maurano, A.; Hamilton, R.; Shuttle, C.G.; Ballantyne, A.M.; Nelson, J.; O'Regan, B.; Zhang, W.; McCulloch, I.; Azimi, H.; Morana, M.; et al. Recombination dynamics as a key determinant of open circuit voltage in organic bulk heterojunction solar cells: A comparison of four different donor polymers. *Adv. Mater.* **2010**, *22*, 4987–4992. [CrossRef] [PubMed]
28. Lange, I.; Kniepert, J.; Pingel, P.; Dumsch, I.; Allard, S.; Janietz, S.; Scherf, U.; Neher, D. Correlation between the open-circuit voltage and the energetics of organic bulk heterojunction solar cells. *J. Phys. Chem. Lett.* **2013**, *4*, 3865–3871. [CrossRef]
29. Garcia-Belmonte, G.; Boix, P.P.; Bisquert, J.; Lenes, M.; Bolink, H.J.; La Rosa, A.; Filippone, S.; Martín, N. Influence of the intermediate density-of-states occupancy on open-circuit voltage of bulk heterojunction solar cells with different fullerene acceptors. *J. Phys. Chem. Lett.* **2010**, *1*, 2566–2571. [CrossRef]
30. Garcia-Belmonte, G.; Juan Bisquert, J. Open-circuit voltage limit caused by recombination through tail states in bulk heterojunction polymer-fullerene solar cells. *Appl. Phys. Lett.* **2010**, *96*, 113301. [CrossRef]
31. Blakesley, J.C.; Greenham, N.C. Charge transfer at polymer-electrode interfaces: The effect of energetic disorder and thermal injection on band bending and open-circuit voltage. *J. Appl. Phys.* **2009**, *106*, 034507. [CrossRef]
32. Credgington, D.; Durrant, J.R. Insights from transient optoelectronic analyses on the open-circuit voltage of organic solar cells. *J. Phys. Chem. Lett.* **2012**, *3*, 1465–1478. [CrossRef] [PubMed]
33. Vandewal, K.; Gadisa, A.; Oosterbaan, W.D.; Bertho, S.; Banishoeib, F.; Van Severen, I.; Lutsen, L.; Cleij, T.J.; Vanderzande, D.; Manca, J.V. The relation between open-circuit voltage and the onset of photocurrent generation by charge-transfer absorption in polymer: Fullerene bulk heterojunction solar cells. *Adv. Funct. Mater.* **2008**, *18*, 2064–2070. [CrossRef]

34. Vandewal, K.; Tvingstedt, K.; Gadisa, A.; Inganäs, O.; Manca, J.V. Relating the open-circuit voltage to interface molecular properties of donor:acceptor bulk heterojunction solar cells. *Phys. Rev. B* **2010**, *81*, 125204. [CrossRef]
35. Piersimoni, F.; Chambon, S.; Vandewal, K.; Mens, R.; Boonen, T.; Gadisa, A.; Izquierdo, M.; Filippone, S.; Ruttens, B.; D'Haen, J.; et al. Influence of fullerene ordering on the energy of the charge-transfer state and open-circuit voltage in polymer:fullerene solar cells. *J. Phys. Chem. C* **2011**, *115*, 10873–10880. [CrossRef]
36. Giebink, N.C.; Wiederrecht, G.P.; Wasielewski, M.R.; Forrest, S.R. Ideal diode equation for organic heterojunctions. I. Derivation and application. *Phys. Rev. B* **2010**, *82*, 155305. [CrossRef]
37. Hendriks, K.H.; Wijpkema, A.S.G.; van Franeker, J.J.; Wienk, M.M.; Janssen, R.A.J. Dichotomous role of exciting the donor or the acceptor on charge generation in organic solar cells. *J. Am. Chem. Soc.* **2016**, *138*, 10026–10031. [CrossRef] [PubMed]
38. Cook, S.; Katoh, R.; Furube, A. Ultrafast studies of charge generation in PCBM:P3HT blend films following excitation of the fullerene PCBM. *J. Phys. Chem. C* **2009**, *113*, 2547–2552. [CrossRef]
39. Bakulin, A.A.; Hummelen, J.C.; Pshenichnikov, M.S.; van Loosdrecht, P.H.M. Ultrafast hole-transfer dynamics in polymer/PCBM bulk heterojunctions. *Adv. Funct. Mater.* **2010**, *20*, 1653–1660. [CrossRef]
40. Ren, G.; Schlenker, C.W.; Ahmed, E.; Subramaniyan, S.; Olthof, S.; Kahn, A.; Ginger, D.S.; Jenekhe, S.A. Photoinduced hole transfer becomes suppressed with diminished driving force in polymer-fullerene solar cells while electron transfer remains active. *Adv. Funct. Mater.* **2013**, *23*, 1238–1249. [CrossRef]
41. Armin, A.; Kassal, I.; Shaw, P.E.; Hambsch, M.; Stolterfoht, M.; Lyons, D.M.; Li, J.; Shi, Z.; Burn, P.L.; Meredith, P.J. Spectral dependence of the internal quantum efficiency of organic solar cells: Effect of charge generation pathways. *Am. Chem. Soc.* **2014**, *136*, 11465–11472. [CrossRef] [PubMed]
42. Li, W.; Hendriks, K.H.; Furlan, A.; Roelofs, W.S.C.; Wienk, M.M.; Janssen, R.A.J.J. Efficient tandem and triple-junction polymer solar cells. *Am. Chem. Soc.* **2013**, *135*, 18942–18948. [CrossRef] [PubMed]
43. Bakulin, A.A.; Dimitrov, S.D.; Rao, A.; Philip, C.Y.; Chow, P.C.Y.; Christian, B.; Nielsen, C.B.; Bob, C.; Schroeder, B.C.; Iain McCulloch, J.; et al. Charge-transfer state dynamics following hole and electron transfer in organic photovoltaic devices. *J. Phys. Chem. Lett.* **2013**, *4*, 209–215. [CrossRef] [PubMed]
44. Yeboah, D.; Singh, J. Dependence of exciton diffusion length and diffusion coefficient on photophysical parameters in bulk heterojunction organic solar cells. *J. Electron. Mater.* **2017**. [CrossRef]
45. Narayan, M.; Singh, J. Photovoltaic contribution of photo-generated excitons in acceptor material of organic solar cells. *J. Mater. Sci. Mater. Electron.* **2017**, *28*, 7070–7076. [CrossRef]
46. Singh, J.; Narayan, M.; Ompong, D. Comparative contributions of singlet and triplet excitons in the performance of organic devices. *Phys. Status Solidi C* **2016**, *13*, 77–80. [CrossRef]
47. Gregg, B.A. Excitonic Solar Cells. *J. Phys. Chem. B* **2003**, *107*, 4688–4698. [CrossRef]
48. Singh, J.; Narayan, M.; Ompong, D.; Zhu, F. Dissociation of charge transfer excitons at the donor-acceptor interface in bulk heterojunction organic solar cells. *J. Mater. Sci. Mater. Electron.* **2017**, *28*, 7095–7099. [CrossRef]
49. Wagenpfahl, A.; Rauh, D.; Binder, M.; Deibel, C.; Dyakonov, V. S-shaped current-voltage characteristics of organic solar devices. *Phys. Rev. B* **2010**, *82*, 115306. [CrossRef]
50. Koster, L.J.A.; van Strien, W.J.; Beek, W.J.E.; Blom, P.W.M. Device operation of conjugated polymer/zinc oxide bulk heterojunction solar cells. *Adv. Funct. Mater.* **2007**, *17*, 1297–1302. [CrossRef]
51. Qia, B.; Wang, J. Open-circuit voltage in organic solar cells. *J. Mater. Chem.* **2012**, *22*, 24315–24325. [CrossRef]
52. Cowan, S.R.; Leong, W.L.; Banerji, N.; Dennler, G.; Heeger, A.J. Identifying a threshold impurity level for organic solar cells: Enhanced first-order recombination via well-defined $PC_{84}BM$ traps in organic bulk heterojunction solar cells. *Adv. Funct. Mater.* **2011**, *21*, 3083–3092. [CrossRef]
53. Meijer, E.J.; de Leeuw, D.M.; Setayesh, S.; van veenendaal, E.; Huisman, B.-H.; Blom, P.W.M.; Hummelen, J.C.; Scherf, U.; Klapwijk, T.M. Solution-processed ambipolar organic field-effect transistors and inverters. *Nat. Mater.* **2003**, *2*, 678–682. [CrossRef]
54. Ebenhoch, B.; Thomson, S.A.J.; Genevicius, K.; Juška, G.; Samuel, I.D.W. Charge carrier mobility of the organic photovoltaic materials PTB7 and $PC_{71}BM$ and its influence on device performance. *Org. Electron.* **2015**, *22*, 62–68. [CrossRef]
55. Lin, J.D.A.; Liu, J.; Kim, C.; Tamayo, A.B.; Proctor, C.M.; Nguyen, T.-Q. Effect of structural variation on photovoltaic characteristics of phenyl substituted diketopyrrolopyrroles. *RSC Adv.* **2014**, *4*, 14101–14108. [CrossRef]

56. Walker, B.; Tamayo, A.B.; Dang, X.; Zalar, P.; Seo, J.H.; Garcia, A.; Tantiwiwat, M.; Nguyen, T. Nanoscale phase separation and high photovoltaic efficiency in solution-processed, small-molecule bulk heterojunction solar cells. *Adv. Funct. Mater.* **2009**, *19*, 3063–3069. [CrossRef]
57. Mandoc, M.M.; Koster, L.J.A.; Blom, P.W.M. Optimum charge carrier mobility inorganic solar cells. *Appl. Phys. Lett.* **2007**, *90*, 133504. [CrossRef]
58. Philippa, B.; Stolterfoht, M.; Burn, P.L.; Juŝka, G.; Meredith, P.; Whitel, R.D.; Pivrikas, A. The impact of hot charge carrier mobility on photocurrent losses in polymer-based solar cells. *Sci. Rep.* **2014**, *4*, 5695. [CrossRef] [PubMed]
59. Koster, L.J.A.; Smits, E.C.P.; Mihailetchi, V.D.; Blom, P.W.M. Device model for the operation of polymer/fullerene bulk heterojunction solar cells. *Phys. Rev. B* **2005**, *72*, 085205. [CrossRef]
60. Würfel, U.; Neher, D.; Spies, A.; Albrecht, S. Impact of charge transport on current voltage characteristics and power-conversion efficiency of organic solar cells. *Nat. Commun.* **2011**, *6*, 6951. [CrossRef] [PubMed]
61. Proctor, C.M.; Kim, C.; Neher, D.; Nguyen, T.Q. Nongeminate recombination and charge transport limitations in diketopyrrolopyrrole-based solution-processed small molecule solar cells. *Adv. Funct. Mater.* **2013**, *23*, 3584–3594. [CrossRef]
62. Oosterhout, D.S.; Ferguson, A.J.; Larson, B.W.; Olson, D.C.; Kopidakis, N. Modeling the free carrier recombination kinetics in PTB7:PCBM organic photovoltaics. *J. Phys. Chem. C* **2016**, *120*, 24597–24604. [CrossRef]
63. Collins, S.A.; Proctor, C.M.; Ran, N.A.; Nguyen, T.-Q. Understanding open-circuit voltage loss through the density of states in organic bulk heterojunction solar cells. *Adv. Energy Mater.* **2016**, *6*, 1501721. [CrossRef]
64. Cravino, A. Origin of the open circuit voltage of donor-acceptor solar cells: Do polaronic energy levels play a role? *Appl. Phys. Phys. Lett.* **2007**, *91*, 243502. [CrossRef]
65. Sun, Y.; Takacs, C.J.; Cowan, S.R.; Seo, J.H.; Gong, X.; Roy, A.; Heeger, A.J. Efficient, air-stable bulk heterojunction polymer solar cells using MoO(x) as the anode interfacial layer. *Adv. Mater.* **2011**, *23*, 2226–2230. [CrossRef] [PubMed]
66. Orlowski, B.A.; Pieniazek, A.; Goscinski, K.; Kopalko, K. Quasi Fermi levels in semiconductor photovoltaic heterojunction. *Acta Phys. Pol. A* **2016**, *129*. [CrossRef]
67. Tuladhar, S.M.; Azzouzi, M.; Delval, F.; Yao, J.; Guilbert, A.A.Y.; Kirchartz, T.; Montcada, N.F.; Dominguez, R.; Langa, F.; Palomares, E.; et al. Low open-circuit voltage loss in solution-processed small-molecule organic solar cells. *ACS Energy Lett.* **2016**, *1*, 302–308. [CrossRef]
68. Baran, D.; Vezie, M.S.; Gasparini, N.; Deledalle, F.; Yao, J.; Schroeder, B.C.; Bronstein, H.; Ameri, T.; Kirchartz, T.; McCulloch, I.; et al. Role of polymer fractionation in energetic losses and charge carrier lifetimes of polymer: Fullerene solar cells. *J. Phys. Chem. C* **2015**, *119*, 19668–19673. [CrossRef]
69. Yao, J.; Kirchartz, T.; Vezie, M.S.; Faist, M.A.; Gong, W.; He, Z.; Wu, H.; Troughton, J.; Watson, T.; Bryant, D.; et al. Quantifying losses in open-circuit voltage in solution-processable solar cells. *Phys. Rev. Appl.* **2015**, *4*, 014020. [CrossRef]
70. Bartynski, A.N.; Gruber, M.; Das, S.; Rangan, S.; Mollinger, S.; Trinh, C.; Bradforth, S.E.; Vandewal, K.; Salleo, A.; Bartynski, R.A.; et al. Symmetry-breaking charge transfer in a zinc chlorodipyrrin acceptor for high open circuit voltage organic photovoltaics. *J. Am. Chem. Soc.* **2015**, *137*, 5397–5405. [CrossRef] [PubMed]
71. Tang, Z.; Liu, B.; Melianas, A.; Bergqvist, J.; Tress, W.; Bao, Q.; Qian, D.; Inganäs, O.; Zhang, F. A new fullerene-free bulk-heterojunction system for efficient high-voltage and high-fill factor solution-processed organic photovoltaics. *Adv. Mater.* **2015**, *27*, 1900–1907. [CrossRef] [PubMed]
72. Ran, N.A.; Kuik, M.; Love, J.A.; Proctor, C.M.; Nagao, I.; Bazan, G.C.; Nguyen, T.-Q. Understanding the charge-transfer state and singlet exciton emission from solution-processed small-molecule organic solar cells. *Adv. Mater.* **2014**, *26*, 7405–7412. [CrossRef] [PubMed]

© 2017 by the authors. Licensee MDPI, Basel, Switzerland. This article is an open access article distributed under the terms and conditions of the Creative Commons Attribution (CC BY) license (http://creativecommons.org/licenses/by/4.0/).